[CANCER RESEARCH 58, 5866-5869, December 15, 1998]

Primary Tumor Size-dependent Inhibition of Angiogenesis at a Secondary Site: An Intravital Microscopic Study in Mice[1]

Axel Sckell,[2] Nina Safabakhsh,[3] Marc Dellian,[4] and Rakesh K. Jain[5]

Department of Radiation Oncology, Massachusetts General Hospital, Harvard Medical School, Boston, Massachusetts 02114

ABSTRACT

Some primary tumors are capable of suppressing the growth of their metastases by presumably generating antiangiogenic factors such as angiostatin. We hypothesized that the amount of inhibitor(s) released by a tumor increases with tumor growth. We tested this hypothesis by evaluating the relationship between the size of a primary tumor and its ability to inhibit angiogenesis at a secondary site. Furthermore, we characterized the effects of the primary tumor on physiological properties of newly formed vessels at the secondary site. Angiogenesis and physiological properties were measured using intravital microscopy of angiogenic vessels in the gels containing basic fibroblast growth factor placed into cranial windows of immunodeficient mice bearing human prostatic carcinoma (PC-3) in their flank. The PC-3 tumor inhibited angiogenesis in the gels, and surgical resection of tumor reversed this inhibition. The inhibition of angiogenesis 20 days after gel implantation (range, 0–83%) correlated positively ($r = 0.625$; $P < 0.008$) with the tumor size on the day of gel implantation (range, 19–980 mm^3). The primary tumor also suppressed leukocyte-adhesion in angiogenic vessels, thus helping them evade the immune recognition. These results provide an additional rationale for combining antiangiogenic treatment with local therapies.

INTRODUCTION

Although complete removal of primary tumors normally is the most effective therapy to reduce the risk of metastatic disease, in certain cases removal of primary tumors is accompanied by a sudden accelerated growth of preexisting metastases at secondary sites (1). Growth of metastases can also be inhibited by tumor mass (2). Furthermore, the growth of a second tumor graft can be hindered by a primary tumor (3). Based on these observations, Folkman and co-workers (4) proposed the following hypothesis: a primary tumor, although capable of stimulating its own vascular bed, can inhibit angiogenesis in the vascular bed of a metastasis or other secondary tumor (4). O'Reilly *et al.* (4, 5) have proven this hypothesis by discovering angiostatin (4) and endostatin (5). These substances specifically inhibit endothelial cell proliferation *in vitro*. They also inhibit angiogenesis *in vivo* not only in tumors but also in angiogenic gels implanted in the cornea of mice (4–6).

We propose here that the amount of angiogenesis inhibitors generated by a primary tumor should increase with tumor size. Therefore, the extent of angiogenesis inhibition at a secondary site should increase with tumor size. A prerequisite to test this hypothesis is the availability of an assay that permits *in vivo* quantification of both angiogenesis inhibition and tumor size. We have recently developed such an assay (7, 8). In this assay, a gel containing bFGF[6] is placed in the cranial window implanted in a mouse. Using intravital microscopy, we can measure angiogenesis and physiological properties of the newly formed vessels in the gel. Thus, we can obtain a better understanding of physiological and pathophysiological events during angiogenesis inhibition at a secondary site. We designed this study to test the following hypotheses: (*a*) the size of the primary tumor correlates with its antiangiogenic potency at a secondary site; (*b*) removal of the primary tumor reverses its antiangiogenic effects; and (*c*) the primary tumor adversely affects the hemodynamics, leukocyte-endothelium interaction, and microvascular permeability of newly formed vessels in the gel.

MATERIALS AND METHODS

Animal Model, Anesthesia, Surgical Techniques, and Tumor Implantation. The experiments were performed in SCID mice (age, 6–10 weeks; mean body weight, 25.0 ± 3.2 g) bred and housed in our defined flora animal colony. A mixture of ketamine hydrochloride (Ketalar; Parke-Davis, Morris Plains, NJ; 100 mg/kg body weight) and xylazine (Xyla-Ject; Phoenix Pharmaceutical, St. Joseph, MO; 10 mg/kg body weight) was used as anesthesia. In one set of male SCID mice (PC-3 mice), a piece (≈1 mm in diameter) of a human hormone-independent prostatic carcinoma (PC-3; Ref. 9) was implanted s.c. into the right flank. In controls, no tumors were implanted. To facilitate surgical resection of tumors *in toto* at a later time, tissue-isolated tumors were grown in four female SCID mice. These tumors are connected to the host-vasculature with a single ovarian artery and a single ovarian vein. To this end, the left ovary was positioned s.c. and injected with a 0.03-ml slurry of minced PC-3 tissue in HBSS (H-9269; Sigma Chemical Co., St. Louis, MO) into its fat pad (10). A stretched paraffin film (Parafilm; American Can Company, Greenwich, CT), wrapped around the ovary, prevented infiltrative tumor growth. In all animals, the preparation of the cranial window was performed as described earlier (11).

Angiogenesis Assay. The preparation of the angiogenic gel and its implantation into the cranial window have been described in detail elsewhere (7). In brief, 20 μl of a gel containing 60 ng of human recombinant bFGF (Life Technologies, Inc., Gaithersburg, MD) was sandwiched between two square pieces of nylon mesh (≈2.5 × 2.5 mm; Tetko, Briarcliff Manor, NY) and placed on the pia mater inside the cranial window. bFGF was dissolved in 2.4 μl of 0.1% BSA (BSA; Sigma), 6.5 mg of aluminum sucrose octasulfate (sucralfate; courtesy of BM Research a/s, Værløse, Denmark), and 17.6 μl of type I collagen (Vitrogen 100; Collagen Corp., Palo Alto, CA) neutralized previously to pH 7.4 by the addition of 1 part of sodium bicarbonate (11.76 g/l) and 1 part of 10× minimal essential medium (Life Technologies, Inc.) to 8 parts Vitrogen 100. The mesh contained 25 to 35 squares with 300-μm interval.

Quantification of Angiogenesis. For quantification of angiogenesis, the anesthetized animal was placed under a stereomicroscope (SMZ-1; Nikon, Tokyo, Japan) with epi-illumination and 12.5-fold magnification (7). The angiogenic response (R) in the gel, expressed in percentage, was calculated as the ratio between the number of squares of the top nylon mesh containing at least one newly formed vessel (N_{ves}) and the total number of squares (N_{tot}): $R = 100 \times N_{ves}/N_{tot}$ [%]. The inhibition of angiogenesis on day 20 after gel implantation (I) was calculated as follows: $I = 100 - R$ [%].

Intravital Microscopy and Permeability Measurement. *In vivo* microscopy was performed using a microscope with epi-illumination (Axioplan;

Received 7/2/98; accepted 10/15/98.

The costs of publication of this article were defrayed in part by the payment of page charges. This article must therefore be hereby marked *advertisement* in accordance with 18 U.S.C. Section 1734 solely to indicate this fact.

[1] Supported by National Cancer Institute Outstanding Investigator Grant R35-CA56591 (to R. K. J.). M. D. and A. S. are recipients of Feodor Lynen-Fellowships from the Alexander von Humboldt-Foundation, D-53173 Bonn, Germany.

[2] Present address: Department of Orthopedic Surgery, Inselspital, University of Berne, CH-3010 Berne, Switzerland.

[3] Present address: Department of Internal Medicine, Temple University Hospital, Temple University, Philadelphia, PA 19140.

[4] Present address: Department of Otorhinolaryngology, Head and Neck Surgery, Klinikum Grosshadern, University of Munich, D-81366 Munich, Germany.

[5] To whom requests for reprints should be addressed, at Department of Radiation Oncology, COX-7, Massachusetts General Hospital, Boston, MA 02114.

[6] The abbreviations used are: bFGF, basic fibroblast growth factor; SCID, severe combined immunodeficient; Rho-BSA, tetramethylrhodamine-labeled BSA.

Zeiss, Oberkochen, Germany) equipped with a ×20 long-working-distance objective (LD Achroplan, ×20/0.40 korr; Zeiss) and a fluorescence filter set (Omega Optical, Brattleboro, VT). For off-line analysis, regions of interest were recorded on video tapes using a S-VHS videocassette recorder (SVO-9500 MD; Sony, Tokyo, Japan) and a regular charge-coupled device (CCD; AVC-D7; Sony, Tokyo, Japan) or intensified CCD video camera (C2400-68; Hamamatsu Photonics K.K., Hamamatsu, Japan). FITC-labeled dextran (Sigma; M_r 2,000,000; 0.1 ml of a 5% solution in 0.9% NaCl as a plasma marker) and rhodamine 6G (Molecular Probes, Eugene, OR; 0.04 ml of a 0.05% solution in 0.9% NaCl as a fluorescence dye to label WBC *in vivo*) were injected i.v. to visualize the microcirculation and to measure leukocyte-endothelium interaction, respectively. The effective permeability (P) to tetramethylrhodamine-labeled BSA (Rho-BSA; Molecular Probes; 0.8 mg/ml PBS) of newly formed vessels in the angiogenic gels was measured as described previously (11, 12). The fluorescence intensity of one selected area per animal was measured with a photomultiplier (9203B; Thorn EMI, Rockaway, NJ) before and 1, 3, 5, 7, 9, 11, 14, 17, and 20 min after i.v. injection of a 0.12 ml bolus of Rho-BSA.

Off-Line Analysis of Microhemodynamics and Leukocyte-Endothelium Interaction. Inconsistency in microhemodynamic parameters can stem from mechanical or morphological properties of vessels. To avoid this problem, we chose only confluent, venous-like 100-μm vessel segments with a straight course and similar diameters (15.5 ± 2.3 μm) from five to eight regions selected randomly per animal and time of investigation. Each of these regions was recorded for 30 s on video tape for the evaluation of leukocyte-endothelium interaction and for 60 s for hemodynamic measurements. Internal diameters (D) in μm and RBC velocity (v_{RBC}) in μm/s were measured using a digital video image-shearing monitor (model 908; IPM, San Diego, CA) and a four slit photometric analyzer (model 208C; IPM), respectively, both connected to a personal computer (IBM PS/2, 40SX; Computerland, Boston, MA). The number of sticking leukocytes (N_S) is expressed as the density of cells (WBC_S) firmly adhering to the inner surface of the investigated 100-μm vessel segment: $WBC_S = 10^6 N_S/(\pi \times D \times 100)$ [cells/mm^2]. Rolling leukocytes are defined as a population of cells temporarily interacting with the vessel wall and thus having a velocity at least 50% smaller than v_{RBC}. Rolling count (WBC_R) is given as a percentage: $WBC_R = 100 \times N_R/N_{WBC}$ [%], where N_R is the number of rolling leukocytes and N_{WBC} is the number of all nonsticking leukocytes. Leukocyte flux (F_{WBC}) was normalized by the cross-section area of the observed microvessel and the observation time (t): $F_{WBC} = 10^6 \times N_{WBC}/[(D/2)^2 \times \pi \times t]$ [cells/mm^2/s]. Apparent wall shear rate (γ) was derived from Poiseuille's law for Newtonian fluid: $\gamma = (v_{RBC}/D) \times 8$ [1/s]. Blood flow (Q) was calculated as follows: $Q = v_{RBC} \times D^2 \times \pi/4000$ [pl/s].

Analysis of Tumor Volume. The size of all tumors implanted was measured using a caliper and corrected for skin thickness (0.5 mm in SCID mice). Tumor volume (V_{TU}) was obtained using the formula: $V_{TU} = \pi/6 \times D_{max} \times (D_{min})^2$ [mm^3], where D_{max} is the maximal tumor diameter and D_{min} is the corresponding perpendicular diameter.

Autopsy and Histology. After sacrificing the animals at the end of experiments, all mice with tissue-isolated tumors as well as some randomly selected mice with PC-3 implanted s.c. were chosen for autopsy to scan for metastases. In these animals, lung, liver, spleen, kidney, heart, and spine were cut in slices for macroscopic investigation. The tissue samples were fixed in 10% formaldehyde and embedded in paraffin. For microscopic investigations, tissue sections were cut and stained with H&E.

Animal Groups. Matched animal groups were used for all experiments. The sequence of measurements between controls and PC-3 mice was selected randomly. In PC-3 mice, the angiogenic gel was implanted when the tumor had reached the desired size. However, before gel implantation in animals, a minimum time of 7 days was allowed to elapse after cranial window preparation to recover from the surgery. Animals with surgery-induced brain bleeding, neurological symptoms, or any sign of inflammation were excluded from the study. To find out whether the effect of PC-3 on angiogenesis response in the gels is reversible, PC-3 was implanted in four animals as tissue-isolated preparation and was removed 2 weeks after gel implantation.

Statistics. Results are presented as means ± SD unless specified otherwise. Data were analyzed statistically using one-way repeated measures ANOVA. As a multiple comparison test, Bonferroni's Method was applied if a normality test was passed and Friedman repeated measures ANOVA as well as Student-Newmans-Keuls Method when normality test failed, respectively. The Pearson Product Moment Coefficient was calculated to analyze correlations. For all tests, Ps <5% were considered significant.

RESULTS

Quantitative Angiogenic Response and Growth of PC-3. In 17 animals bearing PC-3, the inhibition of angiogenesis on day 20 after gel implantation correlated positively with the tumor volume on the day of gel implantation (Fig. 1*A*). Of these 17 animals, angiogenic response in gel assays of 7 PC-3 mice with tumor volumes >205 mm^3 on the day of gel implantation was compared with 22 controls (Fig. 1*B*). Beginning on day 10 after bFGF gel implantation, there was a significant inhibition of angiogenesis in gels in PC-3 mice compared with the control mice. On day 20 after gel implantation, the difference in the angiogenic response between the two experimental groups became 61%. In contrast to controls where angiogenesis significantly increased over time, in PC-3 mice from day 14 onwards the angiogenic response seemed to be suppressed at a constant level. Fig. 1*C* shows the growth of PC-3 of the above-mentioned seven PC-3 mice with tumors >205 mm^3 on the day of gel implantation.

Effect of Tumor Removal on Angiogenic Response. Surgical removal of tissue-isolated PC-3 in four animals 14 days after gel implantation proved that tumor-induced inhibition of angiogenic response to bFGF was completely reversible (Fig. 1*D*). Within 14 days after tumor resection, angiogenesis increased from 29.4 ± 9.1% to 98.8 ± 2.5%.

Autopsy and Histology. In all mice autopsied, macroscopic as well as microscopic investigation of lung, kidney, spleen, liver, heart, and spine did not reveal any sign of tumor metastases as an alternative source for the production of growth-inhibitory substances. All organs investigated showed normal morphology according to the age of the mice.

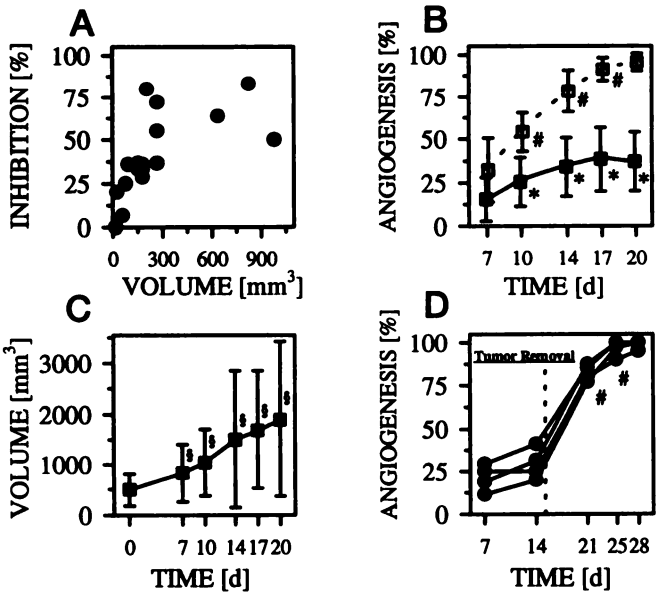

Fig. 1. Analysis of angiogenesis and tumor growth. *A*, correlation of the inhibition of angiogenesis on day 20 after gel implantation in PC-3 mice (n = 17) and their tumor volume at the day of gel implantation (r = 0.625, P < 0.008; ●, single measurements). *B*, angiogenic response in angiogenesis gel assays at different times after gel implantation of controls (□; n = 22) and PC-3 mice (■; n = 7) bearing tumors >205 mm^3 on the day of gel implantation (*, P < 0.05 *versus* controls; #, P < 0.05 *versus* previous measurement). *C*, tumor growth of the PC-3 mice shown in *B* (§, P < 0.05 *versus* all measurements 7 days or earlier). *D*, angiogenic response in angiogenesis gel assays of mice (n = 4) bearing tissue-isolated PC-3 before and after tumor removal (#, P < 0.05 *versus* previous measurement; ●, single measurements). *Bars*, SD.

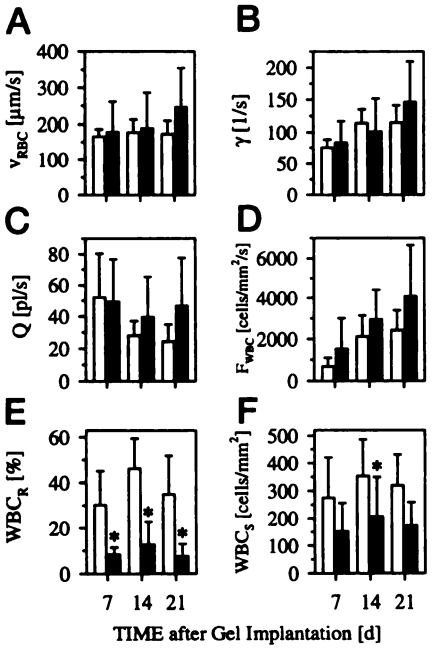

Fig. 2. Microhemodynamics and leukocyte-endothelium interaction in angiogenic vessels of controls (□; $n = 7$) and PC-3 mice (■; $n = 7$). *A*, RBC velocity. *B*, shear rate. *C*, blood flow. *D*, leukocyte flux. *E*, rolling count. *F*, sticking leukocytes. *, $P < 0.05$ *versus* controls. Bars, SD.

Microhemodynamics and Leukocyte-Endothelium Interaction. Analysis of RBC velocity (Fig. 2*A*), shear rate (Fig. 2*B*), and blood flow (Fig. 2*C*) revealed no differences between PC-3 animals and controls over 21 days after gel implantation. At comparable leukocyte flux (Fig. 2*D*) in both groups of animals on days 7, 14, and 21 after gel implantation, rolling count (Fig. 2*E*) in PC-3 mice on average was decreased to 28, 27, and 22% of the corresponding control values. The number of sticking leukocytes in PC-3 mice (Fig. 2*F*) showed a tendency of being reduced, reaching the level of significance only on day 14 after gel implantation. The age of the newly formed vessels in the angiogenesis gel assay had no effect on leukocyte-endothelium interaction.

Microvascular Permeability. No differences were found in microvascular permeability between PC-3 mice and controls at any given time (Fig. 3). In contrast, in both animal groups the very young vessels on day 7 after gel implantation revealed on average 3.4- and 2.0-fold higher permeability to Rho-BSA than older vessels 7 and 14 days later, respectively.

DISCUSSION

The present data show that PC-3 can nonspecifically inhibit angiogenesis at a secondary site. Furthermore, in support of our hypothesis, the size of the primary tumor correlated positively with its antiangiogenic effects at a secondary site. The angiogenesis inhibition was completely reversed after surgical resection of the primary tumor. In PC-3 mice during inhibition of angiogenesis, no changes in microhemodynamic parameters and permeability of newly formed microvessels were detected, whereas leukocyte-endothelium interaction was suppressed.

Animal Model. The *in vivo* angiogenesis gel assay and mechanisms responsible for the bFGF-induced angiogenesis have been discussed in detail elsewhere (7, 13). The present animal model offers a new approach with a high spatial and temporal resolution to perform extensive qualitative and quantitative analysis of antiangiogenic effects induced by a primary tumor at a secondary site. In a similar model where sucralfate pellets containing bFGF were implanted into corneal micropockets of mice, microscopical investigations were performed only on days 5–7 after pellet implantation (6). The present model allows monitoring of the time course of angiogenesis over a time period of up to 4 weeks.

Angiogenic Response. Angiostatin is most likely the substance responsible for the PC-3-induced antiangiogenic effects observed in the present study (14). The positive correlation between tumor volume on the day of gel implantation and inhibition of angiogenesis on day 20 after gel implantation (Fig. 1*A*) gives strong evidence for a dose dependence of the antiangiogenic effects; larger tumors produce higher amounts of antiangiogenic substances. Animals bearing PC-3 smaller than 205 mm^3 showed the same angiogenic response as controls (data not shown). In a few PC-3 mice bearing large tumors, regression of some already established microvessels took place (data not shown). This is in accordance with observations made by O'Reilly *et al.* (5), where systemic administration of endostatin induced regression of primary tumors to dormant microscopic lesions. It was not possible to follow PC-3 mice with tumors >205 mm^3 at the day of gel implantation for >3 weeks. Because of the fast and invasive growth of PC-3, the animals had to be sacrificed after this time. Thus, we could not ascertain as to how long primary tumor-induced suppression of angiogenesis would last. In the present study, surgical removal of tissue-isolated PC-3 abrogated the antiangiogenic effects seen in tumor-bearing animals similar to the observations in some patients and animals (1, 2, 9). Note that the amount of bFGF in gels to induce angiogenesis in our mouse model is relatively much higher than the amount of angiogenic factors produced by early-stage metastases in humans. Therefore, the relatively huge size of PC-3 tumors is necessary to suppress the angiogenic response in the gels sufficiently and, hence, should not be extrapolated on a weight-for-weight basis to the clinical situation in patients.

Microhemodynamics and Leukocyte-Endothelium Interaction. Leukocytes (*i.e.*, mast cells, macrophages, neutrophils, and lymphocytes) are normally associated with angiogenic processes during wound healing, inflammation, and tumor growth (15–17). They have the potential of secreting a wide variety of substances for stimulating angiogenesis and cell proliferation such as proteases, growth factors, and many other monokines (18, 19). Recruitment of leukocytes from circulation into extravascular space is dependent on a multistep cascade of events involving rolling, sticking, and emigration (17, 20, 21). The reduced leukocyte-endothelium interaction in the gels in PC-3 mice at a comparable leukocyte flux in both experimental groups could in part explain why the angiogenic response was suppressed in primary tumor-bearing animals. However, the exact mechanism of action of antiangiogenic substances such as angiostatin and endostatin still remains unclear. RBC velocity, shear rate, and blood flow did not differ between controls and PC-3 mice or over the time within each experimental group. Therefore, it is likely that the factors produced by the primary tumor (*e.g.*, bFGF and transforming growth factor β) induced the reduced leukocyte-endothelium interaction in PC-3 mice

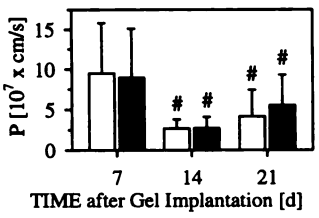

Fig. 3. Microvascular permeability (*P*) of angiogenic vessels in controls (□; $n = 8$) and PC-3 mice (■; $n = 8$). #, $P < 0.05$ *versus* corresponding group on day 7 after gel implantation. *Bars*, SD.

via reduced expression and/or loss of a number of adhesion molecules on the surface of newly formed vessels in the angiogenesis gels. At similar microhemodynamic parameters and leukocyte flux, in controls the number of leukocytes interacting with the endothelium of newly formed microvessels in the angiogenesis gel assay was comparable with data of previous microcirculatory studies in tumors and normal tissues (22). Thus, primary tumor may facilitate evasion of immune recognition at the secondary site by suppressing leukocyte-endothelial interaction.

Microvascular Permeability. In general, microvascular permeability observed in the angiogenesis gels was much higher than in normal tissues and similar or slightly higher than in neoplastic tissues (11, 12, 23, 24). No differences were detected between PC-3 mice and controls. Permeability measurements on days 14 and 21 were comparable with previous measurements on days 12 and 25 in the same system (7). Additionally, we found significantly higher values for this parameter on day 7 after gel implantation *versus* days 14 and 21. Although there was no direct statistical correlation between microvascular permeability and angiogenic response, it seems that vessels at a very early stage of development are more leaky than more mature vessels. This facilitates the extravasation of proteins, which are important for the formation of extracellular matrix for further cell migration (25).

Conclusion. In summary, our model is suitable for investigating the effects of growth-inhibitory factors produced by a primary tumor on angiogenesis at a secondary site. The observed positive correlation between the size of a primary tumor and inhibition of angiogenesis at a secondary site as well as the reversibility of this effect after tumor resection supports the hypothesis that local eradication or regression of certain primary tumors may enhance angiogenesis and thus growth of preexisting metastases elsewhere. Therefore, a cancer patient should benefit from combined local and long-term antiangiogenic follow-up therapies.

ACKNOWLEDGMENTS

We thank Sylvie Roberge for providing the tissue-isolated tumors, Ed Rose and his staff for animal care, and Carol Lyons for help with manuscript preparation.

REFERENCES

1. Sugarbaker, E. V., Thornthwaite, J., and Ketcham, A. S. Inhibitory effect of a primary tumor on metastasis. *In:* S. B. Day, W. P. L. Myers, P. Stansly, S. Garrattini, and M. G. Lewis (eds.), Progress in Cancer Research and Therapy, pp. 227–240. New York: Raven Press, 1977.
2. Prehn, R. T. The inhibition of tumor growth by tumor mass. Cancer Res., *51:* 2–4, 1991.
3. Gorelik, E. Resistance of tumor-bearing mice to a second tumor challenge. Cancer Res., *43:* 138–145, 1983.
4. O'Reilly, M., Holmgren, L., Shing, Y., Chen, C., Rosenthal, R. A., Moses, M., Lane, W. S., Cao, Y., Sage, E. H., and Folkman, J. Angiostatin: a novel angiogenesis inhibitor that mediates the suppression of metastases by a Lewis lung carcinoma. Cell, *79:* 315–328, 1994.
5. O'Reilly, M., Boehm, T., Shing, Y., Fukai, N., Vasios, G., Lane, W. S., Flynn, E., Birkhead, J. R., Olsen, B. R., and Folkman, J. Endostatin: an endogenous inhibitor of angiogenesis and tumor growth. Cell, *88:* 277–285, 1997.
6. Chen, C., Parangi, S., Tolentino, M. J., and Folkman, J. A strategy to discover circulating angiogenesis inhibitors generated by human tumors. Cancer Res., *55:* 4230–4233, 1995.
7. Dellian, M., Witwer, B. P., Salehi, H. A., Yuan, F., and Jain, R. K. Quantitation and physiological characterization of angiogenic vessels in mice: effect of basic fibroblast growth factor/vascular permeability factor and host microenvironment. Am. J. Pathol., *149:* 59–71, 1996.
8. Jain, R. K., Schlenger, K., Höckel, M., and Yuan, F. Quantitative angiogenesis assays: progress and problems. Nat. Med., *3:* 1203–1208, 1997.
9. Kaighn, M. E., Shankar Narayan, K., Ohnuki, Y., Lechner, J. F., and Jones, L. W. Establishment and characterization of a human prostatic carcinoma cell line (PC-3). Invest. Urol., *17:* 16–23, 1979.
10. Kristjansen, P. E. G., Roberge, S., Lee, I., and Jain, R. K. Tissue-isolated human tumor xenografts in athymic nude mice. Microvasc. Res., *48:* 389–402, 1994.
11. Yuan, F., Salehi, H. A., Boucher, Y., Vasthare, U. S., Tuma, R. F., and Jain, R. K. Vascular permeability and microcirculation of gliomas and mammary carcinomas transplanted in rat and mouse cranial windows. Cancer Res., *54:* 4564–4568, 1994.
12. Yuan, F., Leunig, M., Berk, D. A., and Jain, R. K. Microvascular permeability of albumin, vascular surface area, and vascular volume measured in human adenocarcinoma LS174T using dorsal chamber in SCID mice. Microvasc. Res., *45:* 269–289, 1993.
13. Senger, D. R. Molecular framework for angiogenesis: a complex web of interactions between extravasated plasma proteins and endothelial cell proteins induced by angiogenic cytokines. Am. J. Pathol., *149:* 1–7, 1996.
14. Gatley, S., Twardowski, P., Stack, M. S., Patrick, M., Boggio, L., Cundiff, D. L., Schnapper, H. W., Madison, L., Volpert, O., Bouck, N., Enghild, J., Kwaan, H. C., and Soff, G. A. Human prostate carcinoma cells express enzymatic activity that converts human plasminogen to the angiogenesis inhibitor, angiostatin. Cancer Res., *56:* 4887–4890, 1996.
15. Leibovich, S. J., and Ross, R. The role of macrophages in wound repair. A study with hydrocortisone and antimacrophage serum. Am. J. Pathol., *78:* 71–100, 1975.
16. Leek, R. D., Lewis, C. E., Whitehouse, R., Greenall, M., Clarke, J., and Harris, A. L. Association of macrophage infiltration with angiogenesis and prognosis in invasive breast carcinoma. Cancer Res., *56:* 4625–4629, 1996.
17. Jain, R. K., Koenig, G. C., Dellian, M., Fukumura, D., Munn, L. L., and Melder, R. J. Leukocyte-endothelial adhesion and angiogenesis in tumors. Cancer Metastasis Rev., *15:* 195–204, 1996.
18. Sunderkötter, C., Steinbrink, K., Goebeler, M., Bhardwaj, R., and Sorg, C. Macrophages and angiogenesis. J. Leukocyte Biol., *55:* 410–422, 1994.
19. Gullino, P. Prostaglandins and gangliosides of tumor microenvironment: their role in angiogenesis. Acta Oncol., *34:* 439–441, 1995.
20. Butcher, E. C. Leukocyte-endothelial cell recognition: three (or more) steps to specificity and diversity. Cell, *67:* 1033–1036, 1991.
21. Springer, T. A. Traffic signals for lymphocyte recirculation and leukocyte emigration: the multi step paradigm. Cell, *76:* 301–314, 1994.
22. Fukumura, D., Salehi, H. A., Witwer, B., Tuma, R. F., Melder, R. J., and Jain, R. K. Tumor necrosis factor α-induced leukocyte-adhesion in normal and tumor vessels: effect of tumor type, transplantation site, and host strain. Cancer Res., *55:* 4824–4829, 1995.
23. Gerlowski, L. E., and Jain, R. K. Microvascular permeability of normal and neoplastic tissues. Microvasc. Res., *31:* 288–305, 1986.
24. Yuan, F., Chen, Y., Dellian, M., Safabakhsh, N., Ferrara, N., and Jain, R. K. Time-dependent vascular regression and permeability changes in established human tumor xenografts induced by an anti-vascular endothelial growth factor/vascular permeability factor antibody. Proc. Natl. Acad. Sci. USA, *93:* 14765–14770, 1996.
25. Dvorak, H. F., Brown, L. F., Detmar, M., and Dvorak, A. M. Vascular permeability factor/vascular endothelial growth factor, microvascular hyperpermeability, and angiogenesis. Am. J. Pathol., *146:* 1029–1039, 1995.